Chemical Physics Letters 665 (2016) 111–116

Contents lists available at ScienceDirect

Chemical Physics Letters

journal homepage: www.elsevier.com/locate/cplett

Research paper

Design, synthesis and evaluation of a new Mn – Contrast agent for MR imaging of myocardium based on the DTPA-phenylpentadecanoic acid complex

Maxim L. Belyanin [a], Elena V. Stepanova [a,*], Rashid R. Valiev [b,c,d], Victor D. Filimonov [a], Vladimir Y. Usov [e], Oleg Y. Borodin [e,f,g], Hans Ågren [d]

[a] Department of Biotechnology and Organic Chemistry, National Research Tomsk Polytechnic University, 30 Lenin Avenue, Tomsk 634050, Russia
[b] Department of General and Inorganic Chemistry, National Research Tomsk Polytechnic University, 30 Lenin Avenue, Tomsk 634050, Russia
[c] Tomsk State University, Lenin Avenue 36, Tomsk 634050, Russia
[d] Department of Theoretical Chemistry and Biology, Royal Institute of Technology, S-10691 Stockholm, Sweden
[e] Institute of Cardiology, Siberian Branch, Russian Academy of Medical Sciences, Kievskaya St. 111a, Tomsk 634012, Russia
[f] Siberian State Medical University, Mockovskiy trakt 2, Tomsk 634050, Russia
[g] Tomsk Regional Oncology Center, Lenin Avenue 115, Tomsk 634050, Russia

ARTICLE INFO

Article history:
Received 4 October 2016
In final form 20 October 2016
Available online 21 October 2016

Keywords:
MRI-contrast agent
DFT
Molecular docking
Manganese
Gadolinium

ABSTRACT

In the present paper we describe the first synthesis and evaluation of a novel Mn (II) complex (DTPA-PPDA Mn (II)) which contains a C-15 fatty acid moiety that has high affinity to the heart muscle. The complexation energy of DTPA-PPDA Mn (II) evaluated by quantum chemistry methodology indicates that it essentially exceeds the corresponding value for the known DTPA Mn (II) complex. Molecular docking revealed that the affinity of the designed complex to the heart-type transport protein H-FABP well exceeds that of lauric acid. Phantom experiments in low-field MRI the designed contrast agent provides MR imaging comparable to gadopentetic acid.

1. Introduction

Magnetic resonance imaging (MRI) has long been used for effective cardiovascular visualization, accurate determination of ventricular size, mass, function [1,2] pathologies of aorta and myocardium [3–7]. However, metabolic imaging of the heart (ATP, fatty acids, glucose consumption) has not been fully realized in the clinic yet. Therefore, the design of new MRI contrast agents for heart visualization is of particular importance.

Gadolinium-based complexes are typically used for MR imaging despite that free Gd (III) ions are highly toxic as xenobiotic particles [8,9]. Although gadolinium-containing complexes are particularly stable at 20–40 °C [10], their decay to free ions must still be taken into account. As an illustrative example, the widely-used gadopentetic acid may cause a number of side-effects such as nephrogenic systemic fibrosis [11–14].

Manganese-enhanced MRI of the heart has recently gained a growing attention and several manganese-containing complexes have by now successfully been tested in MR imaging experiments [15–18]. Being a natural cellular constituent [19], Mn (II) has similar paramagnetic properties as gadolinium, however, being significantly less toxic [20]. The main idea is that Mn (II) resembles Ca (II), which is a key regulator of myocardial contraction. Mn (II) can 'surrogate' Ca (II) in myocardium calcium exchange and can therefore be used for the evaluation of calcium uptake in the heart. It has thus been established that manganese-enhanced MRI signals reflect changes in the Ca (II) uptake in the myocardium [21,22].

It is known that fatty acids are the most important energy sources for the myocardium and provide up to 90% of its aerobic metabolism via β-oxidation [23]. Radiolabelled *p*-iodophenylpentadecanoic acid (I-PPDA) [24,25] has been approved as a good tracer for SPECT imaging of the myocardium. Kropp and colleagues [26] reported that I-PPDA qualitatively incorporates into endogenous lipids of the heart and metabolizes similarly to the natural fatty acids. Thus, ligands based on phenylpentadecanoic acid (PPDA) chelating Mn (II) can possibly provide both selective delivery of contrast agents to the

* Corresponding author.
E-mail addresses: eline_m@mail.ru, glycoside.m@gmail.com (E.V. Stepanova).

http://dx.doi.org/10.1016/j.cplett.2016.10.058
0009-2614/

myocardium and good MR imaging of the heart muscle. However, conjugates of Mn (II) with PPDA or other fatty acids are unknown in the literature to date. The aim with the present work is to design such a contrast agent, synthesize it for the first time and evaluate its applicability in medicine. The desired ligand contained DTPA-chelating group connected to two PPDA moieties is 15 – (4 – carboxymethyl (2 – carboxymethyl (2 – carboxymethyl (4 – (14-carboxytetradecyl) phenyl carbamoyl methyl) aminoethyl) aminoethyl) – aminomethyl carboxyamido phenyl) – pentadecanoic acid or DTPA-PPDA **4**.

For Mn (II) chelating we chose DTPA due to its favorable properties. DTPA is bifunctional complex one which contains both a good chelating group and chemically reactive functional groups which can be covalently attached to two molecules of PPDA via the amide bond. Multidentate ligand DTPA creates high cation coordination numbers and complexation constants being less rigid in comparison to many other complex ones [27].

2. Materials and methods

2.1. Synthesis of DTPA-PPDA Mn (II)

The ligand DTPA-PPDA **4** was synthesized starting from ω-phenylpentadecanoic acid **1** (Scheme 1). The latter was prepared according to the described procedure [28,29]. Phenyl pentadecanoic acid **1** was nitrated and nitro group of the resulted compound **2** was reduced to give the amine **3**. Condensation of the product **3** with DTPA-bis(anhydride) [30] gave the ligand DTPA-PPDA **4**.

The ligand **4** was prepared as yellowish crystals with the total yield 38%. The ligand was insoluble in chloroform, water and acidic medium. A complete dissolution was observed in absolute boiling ethanol or in $NaHCO_3$ solution at pH > 9.

Complexation of DTPA-PPDA **4** with Mn (II) was carried out by the treatment of DTPA-PPDA with the manganese (II) chloride in $NaHCO_3$ solution. The absence of free Mn^{2+} ions was confirmed by complexometric titration with eriochrome Black [31]. The complexation reaction was successful only if pH 9.5 was achieved. However, this pH is regarded as unacceptably high for the injection formulations [32]. Therefore, the pH of resulted solution has to be adjusted to 8.5–9.0 by 1 M HCl solution after the complete consumption of all Mn (II) ions.

2.2. Calculation details

2.2.1. DFT calculations

Geometry optimization of electronic ground state and the calculation of total energies for all compounds were carried out using Density functional of theory (DFT) with the B3LYP exchange-correlation functional [33]. The DGDZVP basis set [34,35] was used in the case of all structures in the reaction (1) and (3) with Mn (II) described in Section 3.1. The 4f-core ECP53MWB pseudo potential [36] and basis set for 3d-, 6s, and 6p-function for electrons were used for the reaction (2) with Gd (III) and the 6-31G(d,p) basis set was used for other atoms given section in *3.1*. All calculations were performed using the Gaussian-09 software [37] on the Skif TSU supercomputer [38].

2.2.2. Molecular docking

The molecular docking simulations were performed using the AutoDock Vina [39] program and its Autodock tools. Charges and

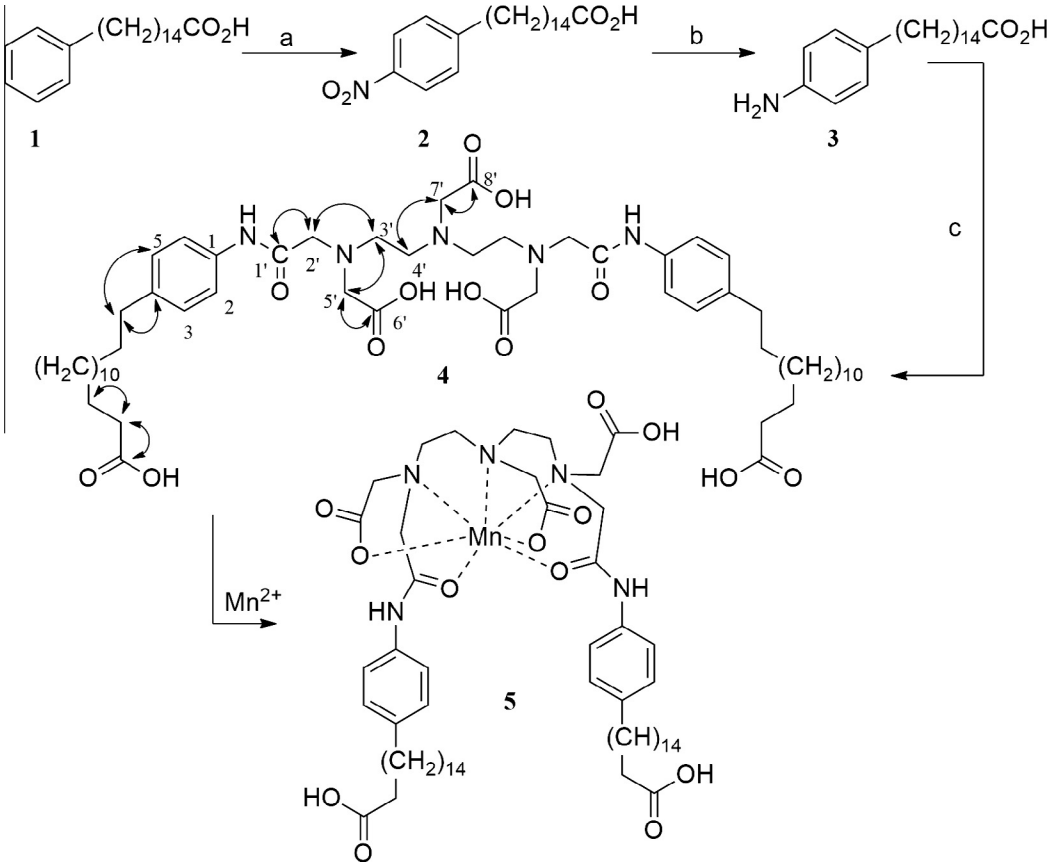

Scheme 1. Synthesis of DTPA-PPDA**4**, its key HMBC correlations and subsequent synthesis of DTPA-PPDA Mn(II) **5** complex. * Reagents and conditions: (a) HNO_3, H_2SO_4, −15 °C, 8 h, (b) H_2, Pd/C 48 h, (c) DTPA-bis(anhydride), which was synthesized according to [30], DMF.

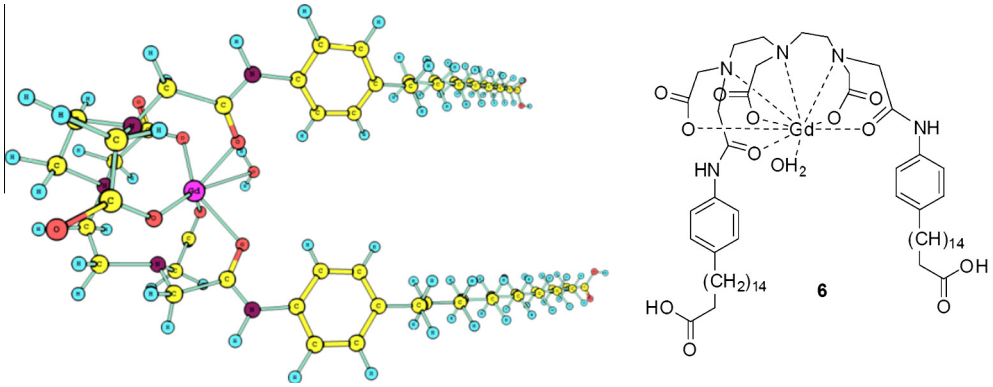

Fig. 1. The structure of DTPA-PPDA Gd (III) **6** complex (Eq. (2)) calculated by DFT method.

Table 1
The calculated complexation (decomposition) energy in kJ/mol at the DFT/B3LYP level of theory.

Ligand	Clc. energy, kJ/mol
DTPA-PPDA Mn (II)	150.624
DTPA Mn (II)	87.864[a]
DTPA-PPDA Gd(III)	384.928

[a] Experimental energy = 83.68 kJ/mol. According to [27], at 20 °C, log K = 15.6. Experimental energy was calculated using the equation: $\Delta G = R \cdot T \cdot \ln K$, or consequently, $\Delta G = 17.5 \cdot \log K$ (kJ/mol).

nonpolar hydrogens were added using default parameters in MGLTools. The size of the docking grid was decreased from default values to include only the inner sphere of the protein. The stringency of docking was set to 8, the default parameter. 3D illustrations were generated and visualized using the PyMol program.

2.3. Phantom experiments in low-field MRI Imaging

MRI experiments were carried out using 'Magnetom Open' (Seimens medical, Germany) at 0.2 T. Phantom experiments were carried out using non-anthropomorphic phantoms – 10 mL glass vessels filled with DTPA-PPDA Mn (II) **5** saline solutions. The solutions were prepared at a range 0.01–2 mM in order to cover a wide range of commonly used T1-weighted measurements using turbo spin-echo sequence with repetition time TR = 420 ms and TE = 15 ms.

The images obtained in T1-weighted sequences were quantified for an average intensity in phantoms of different concentrations and compared with gadopentetic acid of equal concentration to prepare a calibration curve of intensity versus concentration. In the present study we focused on the visualizing properties and did not determine the relaxivity in detail.

3. Results and discussion

3.1. Quantum-chemical calculations

In order to estimate the stability of the DTPA-PPDA Mn (II) complex, we compared it with similar DTPA-PPDA Gd (III) (Fig. 1) complex. It is known that Gd (III) – complexes are used as contrast agents are more stable than the corresponding Mn (II) complexes [10]. For the calculation of the complexation energy of compounds **5**–**6** in water quantum chemical modeling was carried out. The following chemical reactions were simulated:

$$\text{DTPA-PPDA} + \text{Mn(II)} \cdot 6\text{H}_2\text{O} \rightarrow \text{DTPA-PPDA}^{-2}\text{Mn(II)} \cdot 2\text{H}_2\text{O} + 2(\text{H}_3\text{O}^{+}\text{—H}_2\text{O}) \quad (1)$$

$$\text{DTPA-PPDA} + \text{Gd(III)} \cdot 8\text{H}_2\text{O} \rightarrow \text{DTPA-PPDA}^{-3}\text{Gd(III)} \cdot \text{H}_2\text{O} + 3(\text{H}_3\text{O}^{+}\text{—H}_2\text{O}) + \text{H}_2\text{O} \quad (2)$$

The initial structures of DTPA and DTPA-bisphenylamide Mn (II), DTPA-bisphenylamide Gd (III) were taken from the X-ray data in

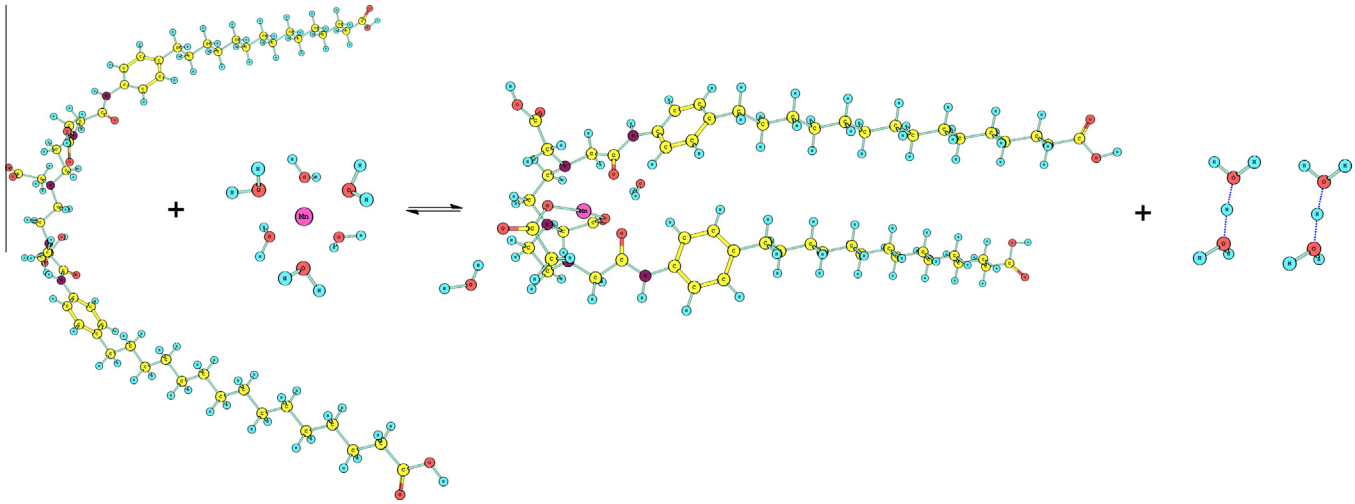

Fig. 2. The reaction of DTPA-PPDA Mn (II) complexation calculated by DFT method.

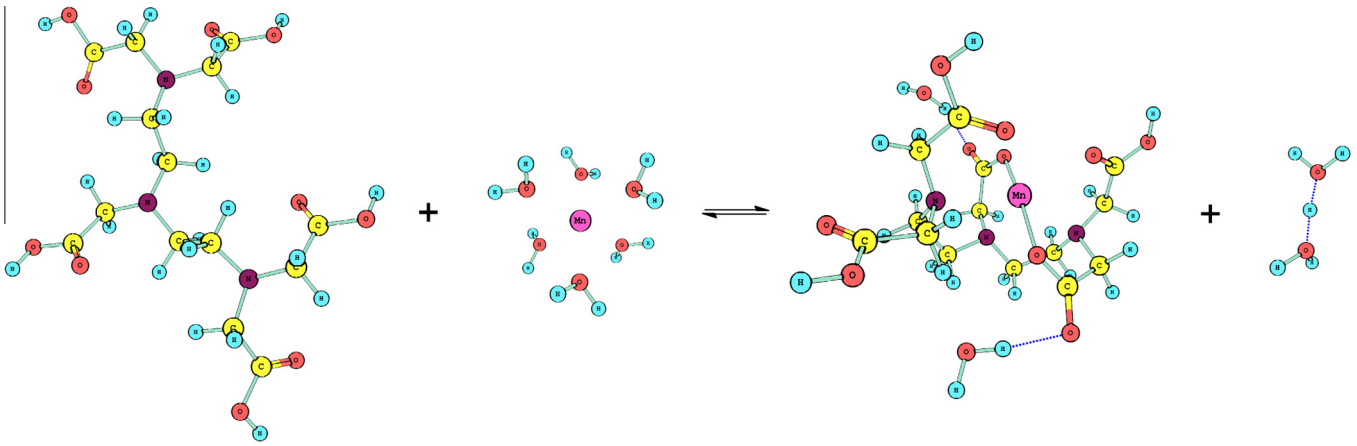

Fig. 3. The reaction of DTPA Mn (II) complexation calculated by the DFT method.

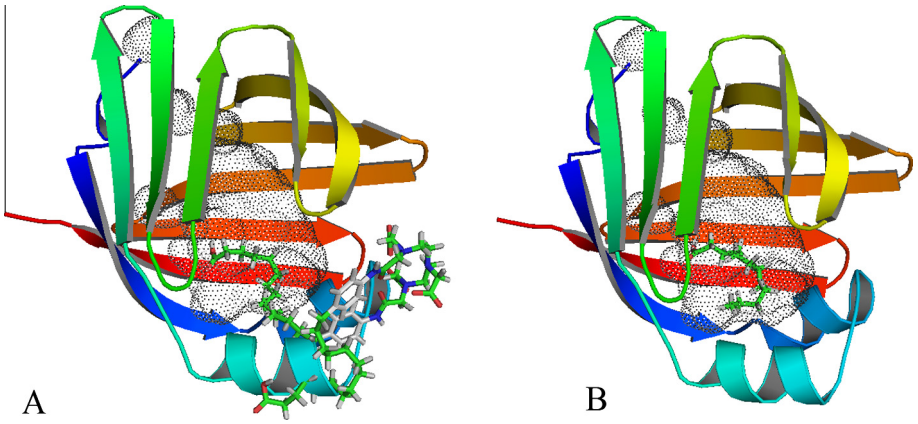

Fig. 4. Molecular docking of H-FABP with A: DTPA-PPDA Mn (II) **5** and B: lauric acid. The inner cavity of the protein is illustrated as dots.

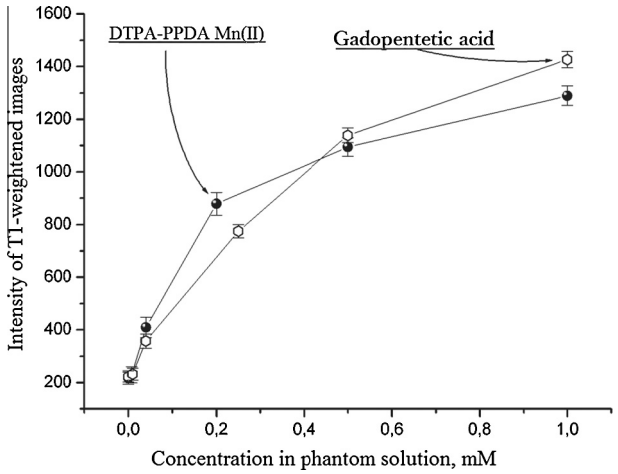

Fig. 5. The intensity of phantoms T1-weighted MR image of different saline solution concentrations of DTPA-PPDA Mn (II) **5** and gadopentetic acid, TR = 400 ms, TE = 25 ms at 0.2 T. ●: DTPA-PPDA; ○: Gadopentetic acid. Data is presented as means SDs ±.

the Ref [40,41] and then augmented by $(CH_2)_{14}COOH$ groups. According to the X-ray analysis, DTPA-bisphenylamide is in the zwitter-ion form in water [40]. As the coordination value of Mn and Gd is 6, respectively, 8 or 9 [42]. We used 6 and 8 molecules of water for the construction of the first water coordination sphere for Mn (II) and Gd (III) ions. According to the X-ray analysis, the complex DTPA Gd (III) contains one water molecule in the coordination sphere. The initial structure of the protonated water cluster (H_3O^+–H_2O) was taken from the Ref. [43].

To validate the theoretical method we performed quantum-chemical calculations for DTPA Mn (II) complex according to the following scheme:

$$DTPA + Mn(II) \cdot 6H_2O \rightarrow DTPA^{-2}Mn(II) \cdot 2H_2O + 2(H_3O^+ - H_2O) \quad (3)$$

The results of complexation energy calculations are combined in Table 1. The complexation energy of DTPA Mn (II) is in a good agreement with experimental data. According to our calculations, complexation energy of DTPA-PPDA Mn (II) **5** complex exceeds DTPA Mn (II) 1.67 times. This allows us to conclude that the C-15 alkyl groups of DTPA-PPDA increase the chelating of Mn (II) as well as change the geometry of the chelating center (Figs. 2 and 3).

The optimized structures of ground state for all compounds in the reaction of DTPA-PPDA Mn (II) complexation are shown in the Fig. 2. The Cartesian coordinates of atoms are given in the supporting information. It can be seen that the Mn (II) cation is coordinated to two amide oxygen atoms with the average Mn—O bond length of 2.29 Å, three tertiary amine nitrogen atoms with average Mn—N bond length 2.50 Å, and two oxygen atoms of deprotonated acetate groups with bond length 2.09 Å. One carboxyl group does not participate in the coordination.

The geometric parameters of DTPA-PPDA Mn (II) are quite similar to those of the simpler complex DTPA Mn (II) (Fig. 3): the average lengths of amide Mn—O 2.38 Å, tertiary Mn—N 2.49 Å and carboxyl Mn—O bonds 2.06 Å. This indicates that the addition of two long-chained hydrophobic tails did not significantly alter the geometry of the chelating center yet the complexation of the manganese ion is enhanced.

It can be seen that after complexation the hydrophobic tails of the resulted DTPA-PPDA Mn (II) complex are moved close one to another in comparison to the initial ligand DTPA-PPDA (Figs. 2 and 3). The hydrophilic DTPA residue becomes more compact which could be an important factor for the transfer of this molecule throughout the myocite membrane.

3.2. Molecular docking

According to recent studies, long-chained fatty acids are incorporated into the myocardium both via passive diffusion and protein-mediated systems such as translocase/CD36 or fatty acid transport proteins [44,45]. Furthermore, a specific heart-type fatty acid binding protein (H-FABP) [46] delivers fatty acids through the cytoplasm to the outer mitochondrial membrane where they metabolize via β-oxidation. Consequently, a scarce affinity to the H-FABP transport protein can be the main hindrance for the heart metabolism of the DTPA-PPDA Mn (II) complex.

In order to estimate the affinity of DTPA-PPDA Mn (II) **5** to H-FABP we performed molecular docking using AutoDock Vina [39]. The structure of the protein was taken from the X-ray analysis Ref. [47]. According to the authors, C12-C18 fatty acids have the best affinity to the active site. Thus, to the validate method, we performed molecular docking of lauric acid and confirmed that the structure of the calculated complex (Fig. 4B) is quite close to that obtained by the X-ray analysis [47]. The results of molecular docking revealed that the affinity of DTPA-PPDA Mn (II) **5** (−6.2 kcal/mol) is even better than calculated for lauric acid (−3.9 kcal/mol). One chain of DTPA-PPDA Mn (II) occupies the same site of H-FABP inner cavity (Fig. 4A) being complementary to the guanidine residue. The DTPA fragment along with the second PPDA chain is adhered to the outer H-FABP aminoacids residues.

3.3. Phantom experiments

The intensity of phantoms T1-weighted MR images of different concentrations of DTPA-PPDA Mn (II) **5** saline solutions compared with gadopentetic acid of equal concentrations is shown in Fig. 5. It can be seen that the T1-weighted images of the former are amplified more than twice from the background even at a concentration 0.04 mmol/L. At 0.2 mmol/L and higher concentrations the amplification exceeded 7–9% of the gadopentetic acid intensity. At 1 mmol/L gadopentetic acid amplified the signal at about 12–15%. Thus, within a concentration range from 0.008 to 1 mmol/L the amplification degree of T1-weighted images with DTPA-PPDA Mn (II) **5** does not yield worse results than gadopentetic acid.

4. Conclusions

In order to search for better contrast agent candidates for heart MRI we have in this work taken advantage of modern quantum chemistry and docking simulation technology in conjunction with MRI phantom experiments. According to quantum chemical DFT calculations of complexation energies, the here studied DTPA-PPDA Mn (II) complex **5** is more stable than the earlier studied DTPA-Mn (II), and consequently, has a reduced decomposition rate. It contains two water molecules in the inner sphere to provide good relaxometric properties [48]. According to molecular docking calculations, DTPA-PPDA Mn (II) can be successfully transferred to mitochondrial membrane to undergo β-oxidation. The designed complex **5** provides MR imaging comparable to gadopentetic acid and, consequently, is a good candidate for further *in vivo* medicinal experiments after the evaluation of its toxicity.

Acknowledgements

V.F. acknowledges the Scientific Programme «Nauka» (N 3.1344.2014).

Appendix A. Supplementary material

Supplementary data associated with this article can be found, in the online version, at http://dx.doi.org/10.1016/j.cplett.2016.10.058.

References

[1] R.A. Takx, A. Moscariello, U.J. Schoepf, J.M. Barraza, J.W. Nance, G. Bastarrika, C. Fink, Eur. J. Radiol. 81 (4) (2012) e598.
[2] Y. Okuhata, Adv. Drug Deliv. Rev. 37 (1) (1999) 121.
[3] P. Sparrow, D.R. Messroghli, S. Reid, J.P. Ridgway, G. Bainbridge, M.U. Sivananthan, Am. J. Roentgenol. 187 (2012) W630, http://dx.doi.org/10.2214/AJR.05.1264.
[4] C.J. François, M.P. Hartung, S.B. Reeder, S.K. Nagle, M.L. Schiebler, J. Magn. Reson. Imag. 37 (6) (2013) 1290.
[5] A. Gotschy, M. Niemann, S. Kozerke, T.F. Lüscher, R. Manka, Int. J. Cardiol. 193 (2014) 84.
[6] Z. Yang, H. Zheng, T. Zhou, L.F. Yang, X.F. Hu, Z.H. Peng, Y.Z. Jiang, M. Li, G. Sun, Int. J. Cardiol. 190 (2015) 103.
[7] A. Wagner, H. Mahrholdt, T.A. Holly, M.D. Elliott, M. Regenfus, M. Parker, R.M. Judd, Lancet 361 (9355) (2003) 374.
[8] W.P. Cacheris, S.C. Quay, S.M. Rocklage, Magn. Res. Imag. 8 (4) (1990) 467.
[9] A.S. Boyd, J.A. Zic, J.L. Abraham, J. Am. Acad. Dermatol. 56 (1) (2007) 27.
[10] S. Aime, A. Barge, C. Cabella, S.G. Crich, E. Gianolio, Curr. Pharm. Biotechnol. 5 (6) (2004) 509.
[11] A.Z. Khawaja, D.B. Cassidy, J. Al Shakarchi, D.G. McGrogan, N.G. Inston, R.G. Jones, Insights Imag. 6 (5) (2015) 553.
[12] A.M. Chiriac, Reactions 1382 (2011) 17.
[13] G. Javaloyes, Reactions 1406 (2012) 16.
[14] N.B. Nayak, Reactions 1471 (2013) 25.
[15] V.Yu. Usov, M.L. Belyanin, A.I. Bezlepkin, A.A. Churin, T.Yu. Dubskaya, T.L. Vetoshkina, V.D. Filimonov, Eksp. Klin. Farmakol. 76 (10) (2013) 32.
[16] V.Yu. Usov, M.L. Belyanin, G.V. Karpova, O.Yu. Borodin, V.D. Filimonov, Eksp. Klin. Farmakol. 71 (4) (2008) 41.
[17] G.A. Rolla, L. Tei, M. Fekete, F. Arena, E. Gianolio, M. Botta, Bioorg. Med. Chem. 19 (3) (2011) 1115.
[18] S.A. Graves, R. Hernandez, J. Fonslet, C.G. England, H.F. Valdovinos, P.A. Ellison, T.E. Barnhart, D.R. Elema, C.P. Theuer, W. Cai, R.J. Nickles, G.W. Severin, Bioconjugate Chem. 26 (10) (2015) 2118.
[19] G.C. Dismukes, Chem. Rev. 96 (7) (1996) 2909.
[20] S. Fuma, H. Takeda, K. Miyamoto, K. Yanagisawa, Y. Inoue, N. Ishii, C. Sugai, C. Ishii, Z. Kawabata, Bull. Environ. Contam. Tox. 66 (2) (2001) 231.
[21] T.C.C. Hu, R.G. Pautler, G.A. MacGowan, A.P. Koretsky, Magn. Reson. Med. 46 (5) (2001) 884–890.
[22] D.C. Medina, D.M. Kirkland, M.F. Tavazoie, C.S. Springer, S.E. Anderson, Contrast Media Mol. Imaging 2 (5) (2007) 248–257.
[23] K. Yoshinaga, N. Tamaki, Curr. Opin. Chem. Biol. 18 (1) (2007) 52.
[24] S.N. Reske, Eur. Heart J. 6 (Suppl. B) (1985) 39–47.
[25] K.J. Mather, T.R. DeGrado, BBA-Mol. Cell Biol Lip. 1861 (10) (2016) 1535–1543.
[26] J. Kropp, K.R. Ambrose, F.F. Knapp, H.P. Nissen, H.J. Biersack, Nucl. Med. Biol. 19 (1992) 283.
[27] G. Anderegg, F. Arnaud-Neu, R. Delgado, J. Felcman, K. Popov, Pure Appl. Chem. 77 (8) (2005) 1445–1495.
[28] F. Kiuchi, N. Nakamura, M. Saitoh, K. Komagome, H. Hiramatsu, N. Takimoto, N. Akao, K. Kondo, Y. Tsuda, Chem. Pharm. Bull. 45 (4) (1997) 685.
[29] T. Siatra-Papastaikoudi, A. Papadaki-Valiraki, A. Tsantili-Kakoulidou, L. Tzouvelekis, A. Mentis, Chem. Pharm. Build. 42 (2) (1994) 392.
[30] E.R. Andersen, L.T. Holmaas, V. Olaisen, Pat. WO2005/58846 A1, 2005.
[31] A. Hioki, N. Fudagawa, M. Kubota, A. Kawase, Talanta 36 (12) (1989) 1203.
[32] Y.C. Lee, P.D. Zocharski, B. Samas, Int. J. Pharma. 253 (2003) 111–119.
[33] M. Shruti, P. Nitin, S. Narayanasami, J. Phys. Chem. A 105 (46) (2001) 2001.
[34] C. Lee, W. Yang, R.G. Parr, Phys. Rev. B 37 (1988) 785–789.
[35] N. Godbout, D.R. Salahub, J. Andzelm, E. Wimmer, Can. J. Chem. 70 (1992) 560–571.
[36] M. Dolg, H. Stoll, H. Preuss, Theor. Chim. Acta 85 (1993) 441.
[37] M.J. Frisch, G.W. Trucks, H.B. Schlegel, et al., Revision D.01, Gaussian Inc., Wallingford, CT, 2009.

[38] www.skif.tsu.ru.
[39] O. Trott, A.J. Olson, AutoDock Vina: improving the speed and accuracy of docking with a new scoring function, efficient optimization and multithreading, J. Comput. Chem. 31 (2010) 455.
[40] Y.C. Liu, S.L. Ma, Q.L. Guo, J. Zhang, M.Q. Xu, W.X. Zhy, Inorg. Chem. Commun. 8 (6) (2005) 574.
[41] S. Dutta, S.K. Kim, E.J. Lee, T.J. Kim, D.S. Kang, Y. Chang, S.O. Kang, W.S. Han, Bull. Korean Chem. Soc. 27 (2006) 1038.
[42] P. Caravan, J.J. Ellison, T.J. McMurry, R.B. Lauffer, Chem. Rev. 99 (1999) 2293.
[43] M.P. Hodges, D.J. Wales, Chem. Phys. Lett. 324 (2000) 279.
[44] F. Kamp, J.A. Hamilton, Prostaglandins Leukot. Essent. Fatty Acids 75 (3) (2006) 149.
[45] R. Ehehalt, J. Füllekrug, J. Pohl, A. Ring, T. Herrmann, W. Stremmel, Mol. Cell. Biochem. 284 (1–2) (2006) 135.
[46] D. Matsuoka, S. Sugiyama, M. Murata, S. Matsuoka, J. Phys. Chem. B 119 (2015) 114–127.
[47] S. Matsuoka, S. Sugiyama, D. Matsuoka, M. Hirose, S. Lethu, H. Ano, T. Hara, O. Ichihara, R. Kimura, S. Murakami, H. Ishida, E. Mizohata, T. Inoue, H. Ishida, Angew. Chem. Int. Ed. 54 (5) (2015) 1508.
[48] G. Hernandez, R.G. Bryant, Bioconjugate Chem. 2 (6) (1991) 394.